Phosphoric acid doped polymer electrolyte membrane based on radiation grafted poly (1-vinylimidazole-co-1-vinyl-2-pyrrolidone)-g-poly (ethylene/tetrafluoroethylene) copolymer and investigation of grafting kinetics

Hamdani Saidi[*], Habibu Uthman

Centre for Hydrogen Energy, Institute of Future Energy, Universiti Teknologi Malaysia, International Campus, Jalan Sultan Yahya Petra, 54100, Kuala Lumpur, Malaysia

ARTICLE INFO

ABSTRACT

A novel composite membrane containing Phosphoric Acid (PA) for possible application in high temperature Proton Exchange Membrane Fuel Cell (HT-PEMFC) was prepared by radiation-induced copolymerization of 1-vinylimidazole (1-Vlm) and 1-vinyl-2-pyrrolidone (1-V-2-P) onto poly (ethylene-alt-tetrafluoroethylene), ETFE films (ETFE-g-P(1-Vlm-co-1-V-2-P)) followed by protonation through PA doping. The preparation procedure involved three steps: i) Irradiation of ETFE films by an electron beam (EB) accelerator, ii) copolymerization of 1-Vlm-co-1-V-2-P onto the EB-preirradiated ETFE films under selected conditions and iii) acid doping of the grafted ETFE films with PA. The physiochemical properties of the resulted membranes were analysed in terms of degree of grafting (DG), grafting compositions, ionic conductivity, thermal properties and thermal stability using Fourier transform infrared spectroscopy (FTIR) fitted with attenuated total reflectance (ATR) and X-ray photoelectron spectroscopy (XPS), thermogravimetric analysis (TGA), and Differential scanning calorimetry (DSC), respectively. The results showed that the physiochemical properties of the membranes are comparable to Nafion 117 especially their thermal stability. At 120 °C and 0% relative humidity the membrane remained stable at 76% DG and 7.6 mmol repeat polymer unit^{-1} with ionic conductivity of 53 mS cm^{-1}. Overall the characterization tests indicated that the membrane displayed impressive thermos-chemical and physical properties with less water dependency. At 200 °C the membrane remained thermally stable which enhances the membrane's potential application in high temperature proton exchange membrane fuel cell (HT-PEMFC) operating at 100 °C and above. Grafting kinetics of nitrogenous and heterocyclic 1-Vim-co-1-V-2-P onto EB-preirradiated ETFE films were also investigated in conjunction with reaction parameters namely: monomer concentration (M), reaction temperature (RT), and absorbed dose (D). This was achieved by the determination of three kinetic parameters namely: the initial

* *Corresponding author.*
E-mail address: hamdani.kl@utm.my (H. Saidi).

polymerization rate (r_{p0}), characteristics radical recombination rate (γ) and delay time (t_0) respectively. The variation of r_{p0} with D and M allows the determination of the order of dependence of grafting rate (R_g) on D and M which are 2.23 and 3.39 respectively. Activation energy (E_a) was also determined followed by temperature effect investigation in the range of 50—70 °C.

Introduction

Attractive materials for energy and environmental applications are functional polymers (resins and membranes) obtained by radiation induced graft copolymerization (RIGC) of nonpolar and polar monomers onto pre-formed polymers. Enhanced properties possessed by these materials are transferred to the polymer matrices when hydrophilic ionic groups are incorporated during grafting or post-grafting reaction. The availability of large number of polymer/monomer combinations to design functional copolymers with specific properties and tuned compositions prompted the use of RIGC in preparation of such materials [1].

Radiation induced grafting (RIG) is a popular versatile technique for synthesizing new materials at low cost with potential applications for producing membranes with desirable properties which meet proton exchange membrane fuel cell (PEMFC) requirements. By tuning the DG(%) through variation of the reaction parameters such as (D), grafting temperature (GT), grafting time (Gt), (M) and solvent type (Sty), this technique offers the merit of gaining total control over the grafted membrane's composition easily. Moreover, to obtain proton exchange membranes (PEMs) devoid of shaping problem, various monomers of established kinetics such as 4-vinylpyridine, styrene and acrylic acid are available to impart specific ionic moieties to polymer films [1].

To develop alternative proton conducting membranes (PCMs) for high temperature proton exchange membrane fuel cells (HT-PEMFCs), phosphoric acid (PA) doping of radiation grafted precursors (films) has been reported [2] Preparation of high temperature proton exchange membranes (HT-PEMs) for HT-PEMFCs applications developed by grafting 1-VIm and/or 1-V-2-P onto ETFE films, followed by PA doping (nano-impregnation) have been studied extensively [2—21].

Nitrogen containing vinyl monomers, such as, 1-VIm, N-vinyl-2-pyrrolidone (NVP), etcetera have been proposed as alternative grafting monomers in order to establish strong hydrogen bonding between N—H atoms that highly contributes to both durability and ionic conductivity of the membranes used in HT-PEMFCs [20]. Therefore, grafting hydrophilic, heterocyclic and nitrogenous vinyl monomers onto hydrophobic base films, such as, ETFE film can be a way to prepare radiation grafted membranes and irradiation of such grafting system leads to the formation of free radicals on the backbone of the polymer substrate which in presence of monomer molecules can initiate copolymerization. Depending on the membrane stability required for a specific application, the polymer substrate could either be fluorocarbon such as, poly(tetrafluoroethylene-co-hexafluoropropylene) (FEP), ETFE or hydrocarbon, including, polyethylene (PE) [9,10,22—24].

NVP is a non-ionic and hydrophilic monomer [15]. NVP has been used to modify surface properties of various substrates, including: low density polyethylene (LDPE), poly (ether sulfone) (PES), etcetera. Summary of previous studies conducted on NVP grafting onto various substrates by different grafting methods has been reported [15]. NVP has attracted much attention in various fields due to its adhesiveness, low toxicity, biocompatibility, and good film forming characteristics [12,14]. During World War I, the polymerization of NVP received much attention when the Germans made use of saline solutions of the polymer as a blood plasma extender [13]. The DG(%) of NVP was reportedly affected by the material of substrate and the grafting polymerization conditions [15]. Poly (N-vinyl-2-pyrrolidone) (PNVP), was first synthesized in the early 1930's in Germany [13]. It was reported that for tethering PNVP onto various substrate surfaces, γ-ray preirradiation grafting was apparently a more efficient way [15].

The technically most important polymer belonging to the family of poly-N-vinylamides is the PNVP. PNVP occupies a special place in a number of water-soluble polymers. Over the last 71 years, it has attracted the constant attention of the researchers. Exhibition of interesting properties by PNVP is due to the fact that it contains a polar amide group and a nonpolar structure allowing pyrrolidone unit to interact favourably with hydrogen-bonded and polar compounds as well as hydrophobic. It is successful commercially due to its adhesiveness, excellent film-forming characteristic, relative inert behaviour towards acids and salts, unusual complexing ability, low toxicity, biological compatibility and its high resistance to thermal degradation in water. Putting it differently, PNVP possesses a unique combination of biological, chemical and chemico-physical properties [17,18,25]. PNVP has great potential applications in numerous technological and scientific fields, such as, UV-curable bio-adhesives, textile auxiliaries, dispersing agents, pharmaceutical fields, soluble drug carriers, plasma substitutes, and etcetera [11—16].

The fact that NVP-co-N-vinylimidazole (NVIm) interacts by different mechanisms have made them very interesting. To obtain highly functionalized polymers with specific properties, combining these monomers (NVP and NVIm) could be a way [12,14,16]. Vinyl-pyrrolidone (VP) and vinyl-imidazole (VIm) copolymers are highly functionalized polymers which exhibits attractive combinations of different properties derived from the two corresponding homopolymers [17,18].

Solution polymerization and precipitation copolymerization of VIm and VP has been recently reported [17,18]. The effect of NVP-co-propylene oxide (PO), the influence of the

chemical and physical properties on the morphology and structure of this copolymer have been reported [16]. Most recently, RIGC of 1-VIm and 1-V-2-P onto EB-preirradiated ETFE films and subsequent PA doping has been successfully carried out by our research group.

For membrane development, various perfluorinated polymers for example, FEP or partially fluorinated films such as, ETFE film have been used frequently as starting materials. This is as a result of their superior thermal, mechanical and chemical properties. Of all fluorinated films, ETFE film have been used widely in the preparation of radiation grafted PEM for fuel cell because of its inherent stability properties (mechanical and thermal stability). High radiation resistance, ability to form stable radicals and superior resistance to common solvents. It improves grafting kinetics of the grafted membrane more than the perfluorinated polymers and enhances its stability. It is inert, stiffer, tougher, less dense, exhibits creep resistance, higher flexural modulus and higher tensile strength above that of perfluorinated polymers [26–38].

1-VIm was selected to provide basic center (−N=) which resembles that of polybenzimidazole (PBI) to conduct protons at a temperature above 100 °C when protonated by PA nano-impregnation [2,5,7–9,24,30,39–41]. Furthermore, availability of more basic centers (−N=) in both 1-VIm and 1-V-2-P resembling that of PBI to conduct protons at temperatures above 100 °C when protonated by PA doping. Strong hydrogen bond (H-bond) is formed between −N=, a basic center and PA through complexation reaction which prevents PA leakage at high temperatures above 100 °C. Poly (1-VIm-co-1-V-2-P) provided the ETFE matrix with −N−groups capable of forming acid/base complex when doped with PA under controlled and optimized conditions in a post grafting reaction.

Reaction parameters, kinetics of reaction and DG(%) are very important in grafting and doping reactions [42]. For efficient grafting of a particular monomer onto a base film, proper understanding of the kinetics of the reaction is very significant. This is very useful in the determination of the effects of reaction parameters on the final DG(%) and rate of reaction. It also important in ensuring that the desired properties in the obtained membrane are maintained. In addition, it guarantees obtaining reproducible results, robust process and cost-effective production [43]. Peculiar aspects of the free-radical polymerization of 1-VIm have been reported [44]. Recently, there were reports on the effect of reaction conditions on reaction kinetics for RIG of styrene onto ETFE and FEP [30,45], and 4-vinylpyridine (4-VP) onto EB-irradiated ETFE films [1]. Employing empirical and mathematical kinetic models, several studies have been reported addressing the grafting kinetics during preparation of grafted membrane precursors [1,2,30]. Though, optimization of PA doping of poly(1-VIm)-graft-poly(-ethylene-co-tetrafluoroethylene) proton conducting membrane precursor have been reported [2]. But, grafting kinetics of 1-VIm-co-1-V-2-P onto ETFE base film has not been reported.

The aim of this study is to use RIGC to prepare PCMs. That is, ETFE-g-P(1-VIm-co-1-V-2-P)/PA doped membrane based on heterocyclic-nitrogenous monomers such as, 1-V-2-P and 1-VIm. They possess desired properties such as, conductivity, chemical, mechanical and thermal stability. They are operational at high temperature particularly above boiling point of water and satisfy less-water dependent conditions for HT-

PEMFCs. Furthermore, the effects of copolymerizing 1-VIm-co-1-V-2-P on the properties of membrane developed was also investigated. To the best of author's knowledge, this is the first reported copolymerization of these monomers (1-VIm-co-1-V-2-P) in PEMs for the fuel cell application in literature. This study also aims to establish the kinetics of RIGC of 1-VIm-co-1-V-2-P onto EB-preirradiated ETFE films. Taking into consideration the effects of various reaction parameters on the DG(%) and grafting rate. Particularly, in conjunction with reaction parameters namely: M, RT and D.

Experimental

Materials

ETFE films of 125 μm thickness and 1.69 g cm^{-1} density was supplied by Good fellow (Cambridge, UK). 1-VIm of 99% purity (Aldrich, USA), 1-Vinyl-2-pyrrolidone (Fluka, Switzerland) of purity 97% were used without further purification. 37% hydrochloric acid and 85% PA were obtained from JT Bakers (NJ, USA). Deionized water of resistance of 18 MΩ was produced using a purifier (NANOpure, DIamond™, UK) and used in grafting and doping experiments. The gases 99% Nitrogen and Oxygen were supplied by Air Product (Malaysia).

Preparation of membrane precursors/grafted ETFE films

Irradiation of ETFE film

Irradiation of the ETFE films were performed according to the methods and procedures described and reported in literature by the groups [2,5,41]. The ETFE film was cut into samples of known area, carefully washed with ethanol and vacuum dried. The film samples were kept in a thin polyethylene bag sealed under vacuum prior to irradiation by a universal electron beam (EB) accelerator (NHV-Nissin High Voltage, EPS 3000, Cockcroft Walton type, Japan) operated at acceleration voltage of 2 MeV, 3 mA and 10 kGy per pass. The film was irradiated to a total dose of 100 kGy. After irradiation, the film was kept in a low temperature freezer at −80 °C for a day.

Co-grafting reaction (copolymerization)

Co-grafting reaction (copolymerization) was performed according to the methods and procedures described and reported in literature by the groups [2,5,41]. This was carried out by introducing an aqueous mixture of 1-VIm and 1-V-2-P of known concentrations to the EB-preirradiated ETFE film in a special ampoule and subsequently flushed for 30 min with a purified N$_2$ to remove air and then sealed tightly. The ampoule was transferred to a water bath at a temperature of 60 °C to start the reaction. After 24 h, the grafted films were extracted in 0.1 M HCl solution under sonication to remove the poly(1-VIm-co-1-V-2-P) homopolymers and unreacted 1-VIm and 1-V-2-P. The degree of grafting, DG(%) in the grafted films (membrane precursors) was calculated as follows:

$$DG(\%) = \frac{w_g - w_o}{w_o} \times 100 \qquad (1)$$

where, w_o and w_g are the weights of the original and grafted ETFE films, respectively. Five grafted samples with different

DG(%) were obtained using an aqueous 1-VIm and 1-V-2-P, each having concentrations in the range of 10–35 vol%.

Acid doping of grafted ETFE films

Grafting reaction was performed according to the methods and procedures described and reported in literature by the groups [5,46]. The grafted films samples of known weight were doped by placing them in a double-wall glass reactor equipped with stirrer, thermometer, and dip-in capillary to bubble the reaction solution with purified N_2. This was followed by introducing PA solution of known concentration, which was varied in the range of 30–60%. The doping temperature (DT) was controlled to the desired values using a thermal liquid circulated with a thermostatic pump. The doping time (Dt) was varied in the range of 5–7 days. After the desired time, the membranes were removed, washed with deionized water several times and dried in a vacuum oven at 60 °C for 16 h. The dried membranes were weighed and the acid doping level per repeated unit of polymer (X_{PA}) (mmol repeat unit^{-1}) was calculated using equation (2):

$$X_{PA} = \frac{(w_d/100)M_p(1 + w_i)}{M_d[1 - (w_d/100)]w_i}$$ (2)

where, w_d is the mass fraction of the dopant, M_p is the molar mass of polymer repeat unit (g mol^{-1}), w_i is the percentage of weight increase of the grafted ETFE film and M_d is the molar mass of PA (g mol^{-1}).

FTIR spectra analysis

Spectra analysis for the samples was performed using Cary 660 FTIR spectrometer fitted with attenuated total reflectance (ATR). FTIR measurements of samples were recorded on a Cary 660 FTIR spectrometer in a transmittance mode at a frequency range of 4000–400 cm^{-1} with a resolution of 4 cm^{-1}. The spectra of the samples were detected and analyzed using "Agilent Resolutions Pro" software.

XPS measurements

XPS measurements were performed on vacuum dried samples using a Kratos XSAM-HS surface micro-analyzer having Mg Kα X-ray source (30 w, 15 kV and 1253.6 eV) in a fixed analyzer transmission mode under a vacuum of 4.0–10^{-1} Torr. Wide scans in the range of 50–1150 eV were recorded at pass energy of 160 eV with 1.0 eV and dwell time of 0.1 s per step, respectively. High resolution spectra were recorded at 45° take-off angle by a concentric hemispherical energy electron analyzer operating in the constant pass energy mode at 29.35 eV, using a 720-μm diameter analysis. Binding energies of all photoelectron effects were recorded by deducing the changing effect values based on C1s at 284.5 eV for terminal hydrocarbon (–CH). The Gaussian peak fitting parameter with a straight baseline was applied for peak analysis using "Vision" software supplied by Kratos.

Thermogravimetric analysis (TGA)

Thermogravimetric analysis (TGA) of the samples was performed using a Netzsch TG 209 F3 Tarsus Thermogravimetric Analyzer. All the heating runs were made in a temperature range of 50–70 °C at a constant heating rate of 20 °C min^{-1} under N_2 atmosphere at a flowrate of 20 ml min^{-1}. Subsequently, analysis of the thermogravimetric and differential/first derivative (TGA/DTG) curves, thermograms of the samples and thermal stability analysis of the composite membrane was performed using Netzsch Proteus software.

Differential scanning calorimetry (DSC) measurements

Differential scanning calorimetry (DSC) measurements was recorded on a Shimadzu DSC-60 analyzer under N_2 atmosphere in a temperature range of 50–300 °C at a constant heating rate of 20 °C min^{-1}. The degree of crystallinity (X_c) of the grafted ETFE film and PA-doped membrane was calculated by taking the heat of melting of a 100% crystalline polymer (113.4 J g^{-1}) into account and correcting the recorded heat of melting by dividing over the weight fraction of ETFE in the grafted film and PA-doped membrane. The degree of crystallinity (X_c) was estimated from the melting peak as shown in equation (3):

$$X_c = \frac{\Delta H_m}{\Delta H_{m\,100}} \times 100$$ (3)

where, ΔH_m is the heat (enthalpy) of melting of ETFE film obtained from the melting peak area and $\Delta H_{m\,100}$ is the heat (enthalpy) of melting of 100% (fully/perfectly) crystalline ETFE polymer, which is 113.4 J g^{-1} [41,47–50].

The thickness of the membrane was measured using a digital thickness gauge (Mitutoyo, Japan). The level of swelling was measured in deionized water and calculated from the weight difference between the membrane in wet and dry conditions.

Swelling

The membranes were dried at 120 °C overnight and then the weight of the membranes was recorded. The dried membranes were then placed in a closed chamber and subjected to water vapour at various levels of controlled relative humidity. For each level of relative humidity, the membrane was kept for 8 h. Subsequently the membranes were taken out of the chamber and wiped with tissue to remove excess vapour. The weight of the wet membranes was then recorded and the swelling percentage from vapour phase was calculated using Equation (4):

$$\text{Swelling}(\%) = \frac{W_{wet} - W_{dry}}{W_{dry}}.$$ (4)

Where, swelling (%) is the swelling percentage from vapour, W_{wet} and W_{dry} are the weights of the wet membrane and the dry membranes, respectively.

Conductivity measurements

The ionic conductivity of the membrane was measured at a temperature range of 30–120 °C using a 4-probe conductivity cell (BT-175) from BekkTech. (Loveland, CO, USA) equipped with thermocouples and temperature controller as shown elsewhere [2]. The cell was connected to a DC source meter (Keithley 2400, Cleveland, OH, USA) and a humidity control system and the whole set-up was controlled by Lab view software. The set-up for conductivity measurement in this study was the same as shown elsewhere [2]. The membrane

was cut into strips of 3 mm × 350 mm size, which was clamped between the Pt electrodes and placed in an externally insulated conductivity cell. The ionic conductivity (σ, S/cm) was calculated according to the following equation (5):

$$\sigma \left(\text{S}/_{\text{cm}} \right) = L/_{RWT} \tag{5}$$

where, W is the width of the membrane sample (cm), T is the thickness of the membrane sample (cm), R is the resistance (Ω) and L is the distance between probes (cm). The ionic conductivity of ETFE-g-P(1-VIm-co-1-V-2-P) membrane was at 120 °C and 0% relative humidity. That is, without humidification/under dry conditions.

Stability of the membrane

The stability test was performed on membrane by heating the membrane samples in an oven at 120 °C for prescribed period of time. The stability was monitored in terms of variation of ionic conductivity in correlation with acid doping level.

Results and discussion

Kinetic analysis

A simple mathematical model was selected and Equations (6)–(9) below were used to describe quantitatively the influence of grafting parameters on the reaction kinetics. As reported [1,30,45,51], variation of DG(%) as a function of time at different reaction parameters (the kinetic plots/graphs) were fitted into the following Equations (6)–(9):

$$DG(\%) = \frac{r_{p0}}{\gamma} \ln[1 + \gamma(t - t_0)] \tag{6}$$

where, r_{p0}, γ and t_0 represent initial polymerization rate, radical lifetime or radical recombination rate or characteristic radical recombination rate and delay time respectively. Where, r_{p0} is given by

$$r_{p0} = k_p[\mathbf{M}]_0[\mathbf{P}^{\cdot}]_0 \tag{7}$$

γ is defined as

$$\gamma = k_t[\mathbf{P}^{\cdot}]_0 \tag{8}$$

where, k_p is the polymerization rate constant, k_t is the rate constant of bimolecular termination (termination of the radical centers occur by bimolecular reaction between two radicals, they react with each other either by coupling or by disproportionation), $[\mathbf{M}]_0$ is the monomer concentration and $[\mathbf{P}^{\cdot}]_0$ is the initial radical concentration. The activation energy (E_a) was calculated using Arrhenius equation (equation (5)) below:

$$k = Ae^{-E_a/RT} \tag{9}$$

where, k is the rate constant, A is the pre-exponential factor or frequency factor, R is the gas constant (8.314 J K^{-1} mol^{-1}) and T is the absolute temperature in K. Since in this model, the rate constant, k is equal to γ or r_{p0}, therefore, from the plot of the ln (k) or ln (r_{p0}) or ln (γ) against reciprocal of temperature (T^{-1}), E_a can be obtained from the slope ($-E_a/R$).

Effect of absorbed dose

Fig. 1 shows the variation of the DG(%) with the reaction time at various absorbed doses for the graft copolymerization of 1-VIm-co-1-V-2-P onto EB-preirradiated ETFE films. It was observed that the DG(%) increases gradually with an increase in D at a specific time. Furthermore, the DG(%) increases with an increase in reaction time (Rt) at a specific D. There was a steep increment in the grafting rate up to 5 h beyond which it shifts to lower past. Increase in the DG(%) can be attributed to the increase in concentration of the trapped radicals that were formed on the backbone of the ETFE due to increase in D which results in more trapped radicals' participating in the grafting reaction during initiation stage of polymerization and eventually yielding numerous growing chains. The possibility of the DG(%) to rise at slow rate after 5 h is most probably due to the reduction in the amount of monomer molecules available at grafting sites after most of them have been consumed during the first few hours of grafting reaction.

By fitting the experimental data obtained into Equations (6)–(9) above, a value of 2.18 which is R_g dependence on the D was obtained from the slope of the log–log plot for the variation of the initial rate of grafting with the D. This value obtained is exceedingly high compare to the theoretical value of 0.5 reported for the typical free radical polymerization [1,30]. This observation most probably resulted from the '*Chemico-mechanical*' effect. The so-called chemico-mechanical effect can be explained based on the fact that at low radiation doses, active sites are often placed moderately far away from one another. Therefore, copolymerization of 1-VIm-co-1-V-2-P commences and propagates randomly resulting in the formation of discrete domains in the ETFE films. As these domains swell in the grafting medium, parts of the bulk of ETFE backbone are left behind intact at the interface between grafted and ungrafted domains. This causes strains, which results in the rupture of some polymeric chains and creation of new 'radicals' for grafting reaction [1,17,18]. Higher values for the dependence of the R_g on the D than the corresponding theoretical value of 0.5 have also been reported for various monomer combinations [1,30]. It was also suggested that the presence of a certain level of mutual recombination of some trapped radicals as a result of reduction in the mobility of
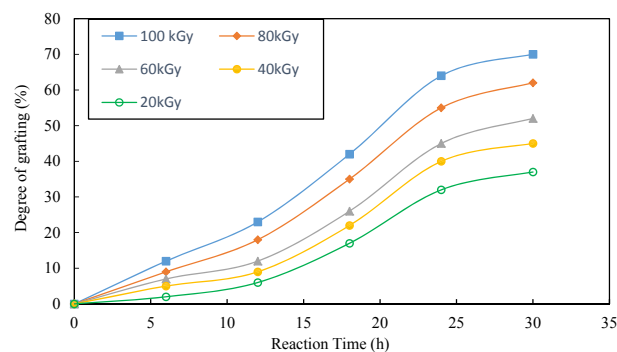

Fig. 1 – Variation of the degree of grafting versus reaction time at different absorbed doses. Grafting conditions are: 1-VIm concentration, 30 vol%; 1-V-2-P concentration, 30 vol%; reaction time 30 h and reaction temperature 60 °C.

polymer chain due to the copolymerization of 1-VIm-co-1-V-2-P crosslinking tendency and the possibility of the occurrence of crosslinking during the irradiation of ETFE films using high energy radiation source might have facilitated the high Rg dependence on D [1,17,18].

From the fitting of the experimental data to the kinetic plots in Fig. 1 in accordance with Equation (2), the values of the three kinetic parameters presented in Fig. 2 were obtained. As D increases, γ and r_{p0} increase. Most likely responsible for the increase in the r_{p0} is the effective utilization of radicals during chain initiation and chain propagation stages. Another reason for the strong dependence of γ on preirradiation dose may be the presence of some inactive radicals which were affected by either homopolymerization or recombination reactions. This trend is in agreement with those reported for the classical solution polymerization and precipitation copolymerization of 1-VIm-co-1-V-2-P [17,18], grafting of 1-VIm onto ETFE and 4-VP onto ETFE [1,41]. The third parameter which is t_0 was observed to have almost a constant value close to 0.4 for all doses and almost independent of the D, this completely agrees with those recently reported [1,30,45,51].

Effect of monomer concentration

In the entire grafting process based on preirradiation technique, the diffusion and reactivity of the monomers are the key parameters. Similarly, homopolymer formation is a side reaction which occurs during grafting reaction that must be dealt with. Hence, it is significant to optimize the initial monomer concentration in order to limit the side reaction in the grafting solution thereby increasing the grafting efficiency and eventually to achieve suitable DG(%) with a low monomer concentration [30]. The variation of DG(%) with reaction time at various monomer concentrations (Ms) for graft copolymerization of 1-VIm-co-1-V-2-P onto ETFE films is shown in Fig. 3. It was observed that with an increase in monomers (1-VIm-co-1-V-2-P) concentration up to 60 vol%, the DG(%) conspicuously increases and at this concentration, a maximum DG(%) of 76% was achieved. As the M increases
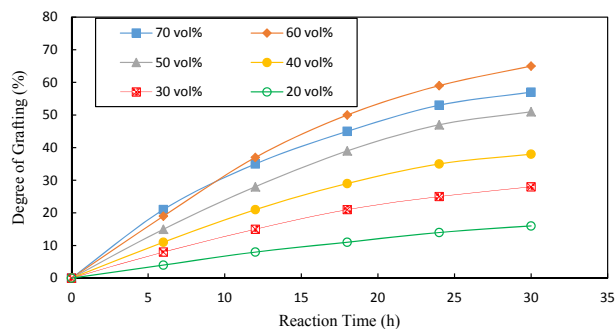

Fig. 3 — Variation of the degree of grafting versus reaction time at different monomer concentrations. Grafting conditions are: absorbed dose, 100 kGy and reaction temperature 60 °C.

further beyond this concentration, the DG(%) declined sharply. Interestingly, at virtually all Ms, the DG(%) was observed to increase with the reaction time and after 10 h it appeared to level-off.

Continuous supply of diffused 1-VIm-co-1-V-2-P molecules that reaches grafting sites and increase in their concentrations in the grafting layers may be responsible for the increase in DG(%) observed with the increase in the monomers concentration. However, there is an enhancement in the homopolymer formation and monomers diffusion across viscous medium onto the grafting sites is hindered at very high concentration of monomers above 60 vol%. Hence, there was a decline in the rise of the DG(%) after the first 10 h. It can be reasonably stated that the increase in the DG(%) with reaction time is due primarily to gradual increase in the amount of monomers diffused to the grafting sites.

This led to a progressive grafting occurring at a slow rate after 10 h than the earlier mentioned 10 h. This continues until when grafting fronts from the sides of ETFE film met at 24 h and saturation is almost achieved. The R_g dependence on the M which gives a value of 3.19 was obtained from the slope of the log–log plot of the variation of the r_{p0} with the M shown in
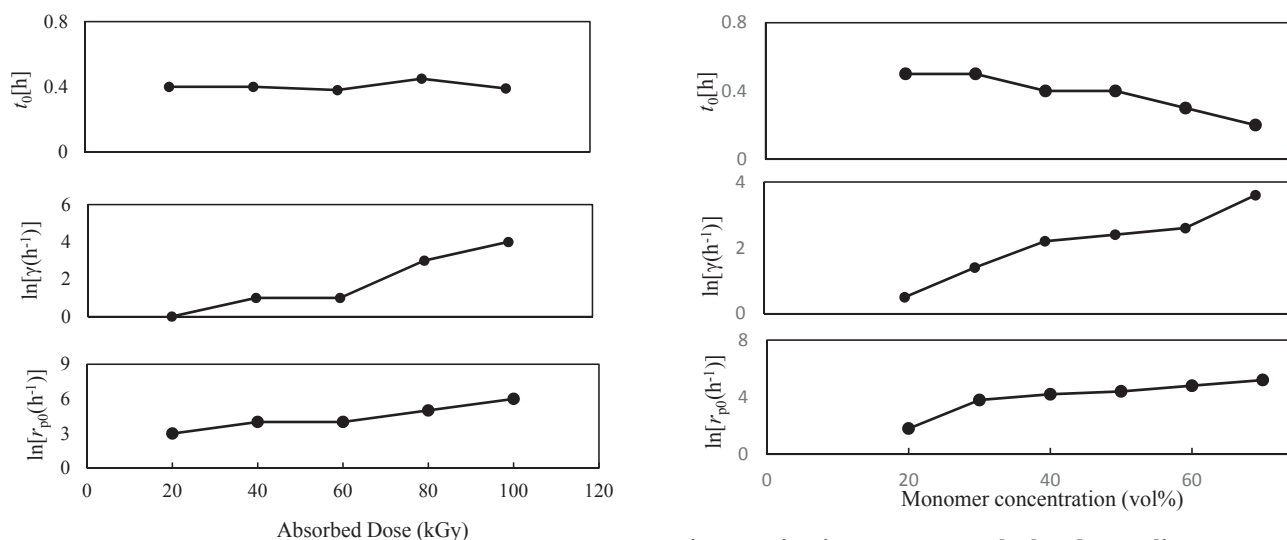

Fig. 2 — Parameters calculated according to Equation (7).

Fig. 4 — Kinetic parameters calculated according to Equation (7).

Fig. 4. This order is not in accordance with the first order dependence of classical free radical polymerization and was found to be 0.3 less than the value reported for 4-VP-*g*-ETFE films [1]. The first order dependence of the grafting rate on M expresses the classical free radical polymerization kinetics. Increase in the viscosity in the grafting sites and extensive homopolymerization during grafted reaction which is known to hinder the monomer diffusion to the radical sites and promote termination by impurities thereby lowering the yielded DG(%) is most probably responsible for such high dependence of the grafting rate on the M and complexity observed.

Fig. 4 shows the kinetic parameters (r_{p0}, γ, t_0) extracted from the curve fitting. As the M increases until 60 vol%, the r_{p0}, increases considerably. The fact that grafting reaction proceeds smoothly as long as the monomer is available at grafting sites and its access to the propagating sites is facilitated can be the basis to explain this observation. Meanwhile, in the beginning, γ changes slightly. Nevertheless, with increase in M above 50 vol%, a dramatic increase in γ was observed and the increase in the recombination and termination reactions or the delay of radicals due to transfer of radicals from the backbone of the ETFE films to the solvent (formation of homopolymer in the grafting solution) may be responsible for this observation. The third kinetic parameter which is t_0 at the beginning increased slightly and above a concentration of 30 vol% (15 vol% 1-VIm and 15 vol% 1-V-2-P) it decreased considerably. At lower concentrations of 1-VIm and 1-V-2-P (20 and 30 vol%), t_0 is higher because of the availability of fewer molecules of monomers (1-VIm-*co*-1-V-2-P) for diffusion to the grafting sites. Whereas, at higher monomer concentrations, due to the availability of more monomer molecules in the grafting sites, there was an enhancement in the progress of the grafting front to the centre of the base film (ETFE film) with shorter induction period. For grafting of 1-VIm-*co*-1-V-2-P onto ETFE films, the kinetic equation (R_g) can be presented in the form expressed in Equation (6) below, based on the results obtained from the variation of the kinetic parameters with the M and D.

$$R_g \alpha \ [M]^{3.39} \ [D]^{2.23} \tag{10}$$

where, M and D are the monomer concentration and absorbed dose, respectively. This Equation (10) above demonstrates that in the present system, grafting kinetics depends on the amount of efficient trapped radicals, concentration of the monomer in the grafting sites, which is determined by the rate of monomer diffusion.

Effect of temperature

Some of the factors that controls grafting include cumulative effect of the monomer diffusion within the bulk of polymer, growing polymer chains' termination and primary radicals' deactivation. The temperature of the grafting reaction is expected to have a significant effect on the achieved DG(%) and on the kinetics of the reaction. Fig. 5 presents the variation of DG(%) with the reaction time (Rt) at different temperatures in the range of 50—70 °C. It was noted that with an increase in RT, the DG(%) increases. And
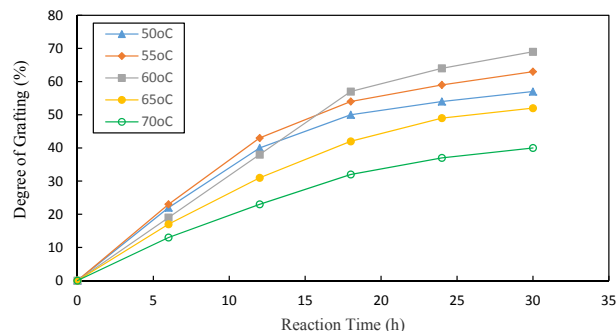

Fig. 5 — Variation of the degree of grafting versus reaction time at different reaction temperature. Grafting conditions are: absorbed dose, 100 kGy; reaction time 30 h; 1-VIm concentration, 30 vol%; 1-V-2-P concentration, 30 vol%.

at 60 °C, maximum DG(%) was achieved after which with further increase in RT, DG(%) decreased considerably. It was also noted that with an increase in Rt, the DG(%) increases and saturation was approached after 15 h. A correspondent increase in the diffusion of monomer within the polymer bulk occurred which enhances monomer accessibility to the grafting sites within the bulk of the polymer as RT increases.

Thus, there was enhancement in the initiation and propagation rates and eventually upon termination, DG(%) increased. Decrease in the DG(%) after 60 °C may be attributed to possible radicals' recombination and formation of homopolymer in the grafting solution hindering monomers' diffusion. The monomer diffusion is reduced by the former, while the latter scavenges for some of the radicals that should ordinarily contribute to initiation reaction. Hence, the final DG(%) obtained decreases despite the apparent increment in the initial grafting rate that was observed at high temperatures. The tendency of the DG(%) to level-off after 15 h most likely resulted from the inward movement of the grafting fronts from both surfaces towards membrane's core. As
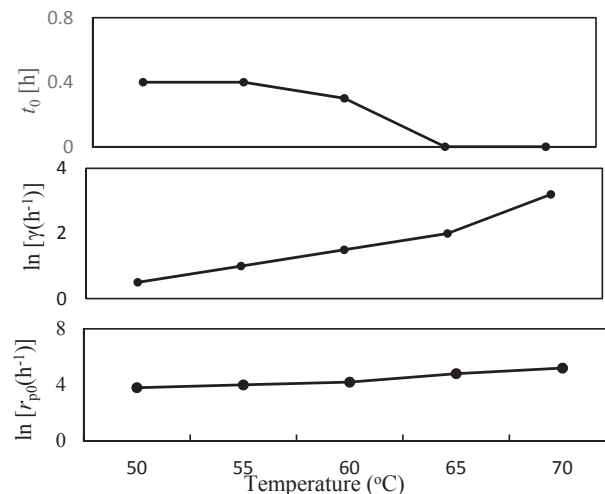

Fig. 6 — Kinetic parameters calculated according to Equation (7).

depicted in Fig. 6, with the increase in temperature range from 50 to 70 °C, r_{p0} was observed to increase significantly. This observation may be ascribed to the enhancement of radical reactivity which led to the increment in initiation and propagation rates which in turn led to increase in 1-VIm and 1-V-2-P diffusion and availability of more of their molecules at higher temperatures in the grafting sites. Mutual recombination of the trapped radicals may be responsible for the drastic increase of γ after 60 °C. In addition, another possible contributing factor to this observation is the bimolecular termination of the graft growing chains which become favourable at high temperatures. The t_0 was observed for temperature range of 50–70 °C, as a consequence of the improvement in the monomer diffusion to the grafting sites, no t_0 is obtained.

Fig. 7 shows the logarithmic plot of the r_{p0} and γ versus the T^{-1}. According to Equation (7) above and using experimental data obtained, the E_a for both the propagation rate (r_{p0}) and termination rate (γ) were calculated from the slope of the Arrhenius plot which equals $-E_a/R$. The E_a calculated for propagation in the temperature range of 50–70 °C is 116.40 kJ mol^{-1}. This E_a value is higher than the E_a obtained for grafting of crosslinked PTFE film (39.7 kJ mol^{-1}) [52], styrene onto various films such as ETFE (98.4 kJ mol^{-1}) [30]. But, this E_a value (116.40 kJ/mol) is closer to the one reported for the grafting of 4-vinylpyridine onto ETFE film (111.41 kJ mol^{-1}) [1]. Similarly, the E_a obtained for the present grafting system is comparatively equally closer to the E_a obtained for co-grafting of α-methylstyrene and methacrylonitrile onto FEP film (101 kJ mol^{-1}) [36]. Strong dependence of grafting on temperature and a low grafting rate is suggested by this moderate value of E_a. The E_a obtained for the recombination rate was 125.71 kJ mol^{-1} which is higher that the E_a obtained for propagation rate. This observation can be used to explain further the increment in the DG(%) at higher temperatures. In both radical decay and initial polymerization rate, there is a similarity in the increasing trends. The latter has its impact on the termination and the final DG(%). While, in same manner, the former affects the propagation of the growing chains. This is probably the main reason for obtaining same maximum DG(%) at the same time intervals (30 h) with the variation of grafting parameters such as, M, RT and D.
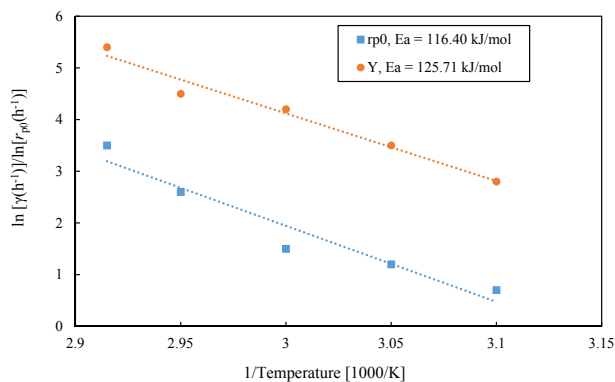
Evidences of grafting (FTIR and XPS spectroscopy)

A membrane with a DG(%) of ~76% was prepared by RIG of an aqueous mixture of 1-VIm and 1-V-2-P of known concentrations onto ETFE films. At 100 kGy absorbed dose, 60 °C reaction temperature and 24 h reaction time. This was followed by a treatment with a 60% PA solution at 100 °C for 5–7 days. To provide an evidence for effective ETFE-g-poly(1-VIm-co-1-V-2-P) formation and PA doping, FTIR analysis was performed on the membrane. The original ETFE films were compared with grafted and PA doped membrane as shown in the FTIR spectra presented in Fig. 8. The bulk composition of the grafted films was determining by FTIR while the probing of the surface of the grafted films was done by ATR and the measurements was performed using a 45° ZnSe crystal (Graseby Specac). The effectiveness of copolymerization of 1-VIm-co-1-V-2-P was proved using FTIR fitted with ATR measurements. The spectrum of ETFE film displayed a number of strong bands in the range of 1000–1400 cm^{-1} resembling C–F of CF$_2$ groups, in addition to a small band at 2915 cm^{-1} representing stretching vibrations of CH$_2$ groups. The grafted films prevailed additional characteristic bands representing –CN groups in the range of 1525–1575 cm^{-1}. The bands at 2750–3150 cm^{-1} and 3200–3650 cm^{-1} were respectively assigned for N–H and C–H of the grafted imidazole rings, which are mostly involved in a network of H-bonding between the imidazole rings and the moisture as expected from their amphoteric behaviour [8,41]. The new absorption band at 1654 cm^{-1} can be assigned to the C=O stretching vibration of the amide group in the pyrrolidone ring. Another two new peaks were also observed at about 1292 cm^{-1} and 1181 cm^{-1} ascribed to the stretching vibration of C–N bond and the stretching vibration of C–C of pyrrolidone ring. This trend is in good agreement with the behaviour of other PA membranes reported in the literature and can be attributed to the formation of H-bonding and hydrogen phosphate groups [5,9,41,53].
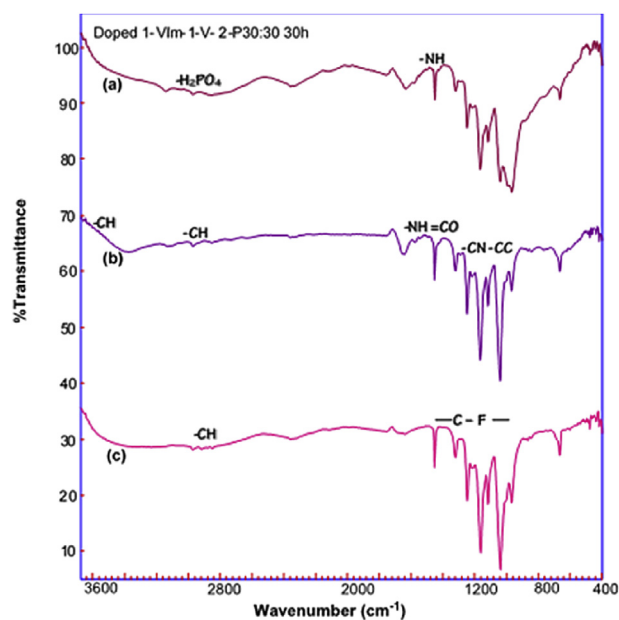

Fig. 7 – Plots of characteristic radical recombination rate, γ and initial polymerization rate, r_{p0} against the inverse temperature.

Fig. 8 – FTIR spectra of (a) PA doped membrane, (b) 76% grafted ETFE film and (c) original ETFE film.

Therefore, suggesting reasonable mechanism shown in Fig. 9 for the PA nanoimpregnated (doped) membrane synthesized in this study is in order.

Nitrogenous-heterocyclic 1-V-2-P and 1-VIm monomers were selected to provide a basic center (−N=) resembling that of PBI to conduct protons at temperatures above 100 °C when protonated by PA doping. Compare to grafting of only 1-VIm onto ETFE base films followed by PA-doping. When 1-VIm-co-1-V-2-P were grafted onto ETFE films and doped with PA. It was observed that the presence of more basic center (−N=) provided by both 1-VIm and 1- V-2-P resembling that of PBI to conduct protons at temperatures above 100 °C when protonated by PA doping is most probably responsible for increased DG(%), DL and proton conductivity. Strong hydrogen bond (H-bond) is formed between −N=, a basic center and PA through complexation reaction which prevents PA leakage at high temperatures above 100 °C. Furthermore, P(1-VIm-co-1-V-2-P) grafts provided the ETFE matrix with −N− groups capable of forming acid/base complex when doped with PA under controlled and optimized conditions in a post grafting reaction. This probably contribute to the increase in DG(%), DL and proton conductivity observed.

A plot of mass (weight) change in a substance as a function of temperature or time under a controlled atmosphere is termed thermogravimetric (TGA) curve. For investigating thermal behaviour of materials such as membrane and determining the kinetics of the thermal degradation, it is a useful technique. While, the differential/first derivative thermogravimetric (DTG) curve, which illustrates the rate of mass (weight) loss as a function of temperature, is the first derivative $[d(w\%)/dt]$ (%/min) of the TGA plot [54,55] TGA and corresponding DTG curves of the original ETFE film, grafted ETFE film and corresponding PA doped membrane are shown in Figs. 10 and 11. In the determination of the onset temperature of degradation (T_{onset}), mass loss rate, residual mass and peak temperature (T_p), DTG curves often assists [5,28,49].

The thermal stability of the developed membrane was investigated and compared with the grafted and original ETFE films using TGA technique. Thermograms obtained were presented in Fig. 10. Grafted ETFE film showed a three-step degradation pattern at 129, 328 and 439 °C respectively due to the dehydration of moisture traces involved in H-bonding with the basic imidazole and pyrrolidone rings, decomposition of P(1-VIm-co-1-V-2-P) grafts and decomposition of ETFE molecular chains. While the original ETFE film had a single-step degradation pattern at 439 °C. As indicated by the transitions at 328 and 439 °C respectively. It is interesting to note that the grafted P(VIm-co-1-V-2-P) were found to be incompatible with ETFE backbone leading to the formation of phase separated domains in the grafted films.
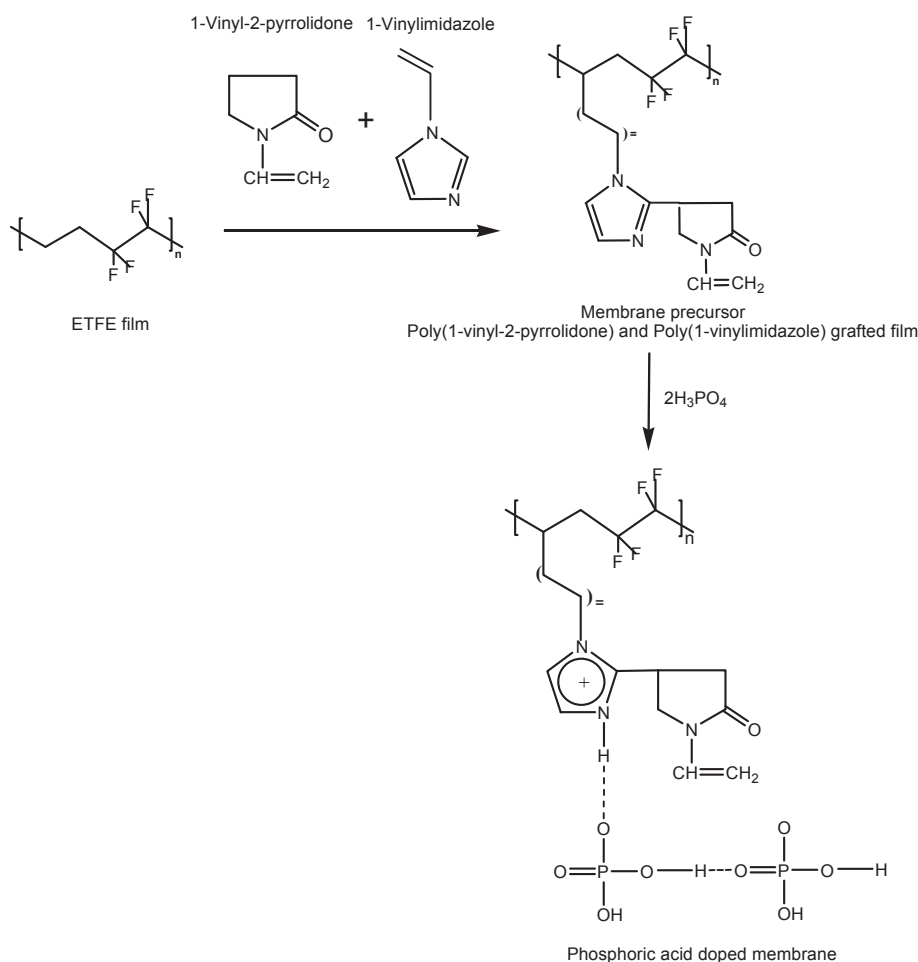

Fig. 9 — Reasonable mechanism of preparation of PEMs by RIG of 1-VIm and 1-V-2-P onto ETFE film followed by PA doping.
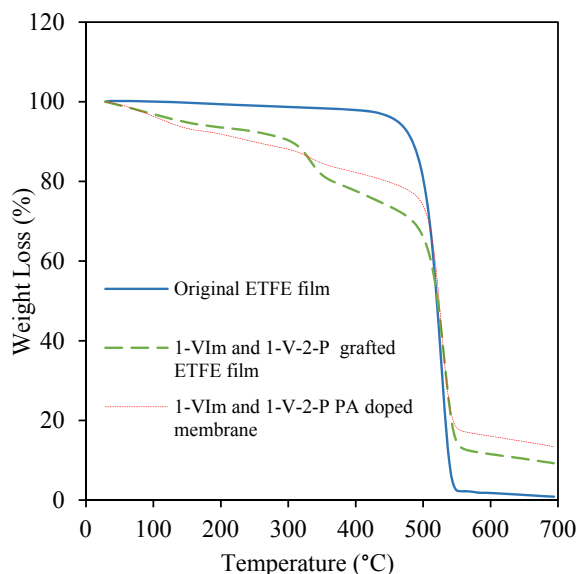
Fig. 10 − TGA thermograms of (a) original ETFE film, (b) 76% grafted ETFE film and (c) corresponding PA doped membrane.
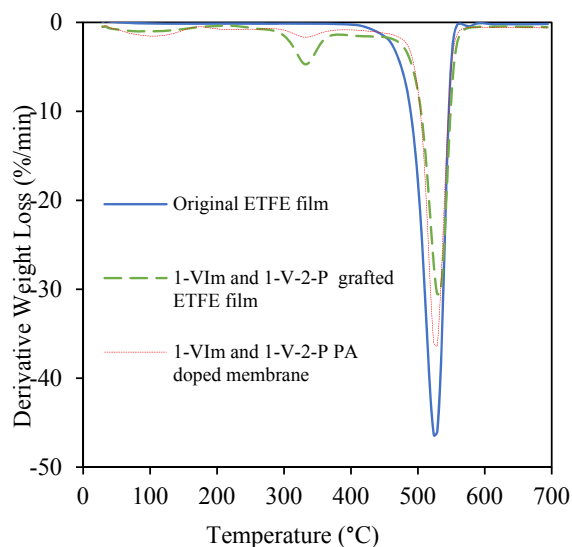

Fig. 11 − DTG thermograms of (a) original ETFE film, (b) 76% grafted ETFE film and (c) corresponding PA doped membrane.

Difference in the nature of the ETFE-g-P(1-VIm-co-1-V-2-P) which are fully amorphous compare to the crystalline fraction of (semicrystalline) ETFE matrix can be responsible for the incompatibility trend observed between them. Since it is well-known that grafting does occur in amorphous regions close to the crystalline lamellae. Mechanical properties ETFE film depends on the X_c since it is a semicrystalline polymer. X_c, size and orientation of the molecular chain determines the overall properties of semicrystalline polymers. The thermograms of the PA doped membrane displayed a three-step degradation pattern which started at 124 °C by dehydration followed by

continuous decomposition caused by de-polymerization of the ETFE-g-P(1-VIm-co-1-V-2-P) and removal of PA at 324 °C and subsequent decomposition of ETFE molecular chains at 424 °C.

The onset temperature of degradation (T_{onset}) for the PA doped membrane was found to be 5 °C lower than (124 °C) that of the grafted film (129 °C) due to the higher moisture content in the PA doped membrane. The reason most likely responsible for the absence of any distinction between their decomposition transitions is the closeness in the values of thermal degradation temperatures of P(1-VIm-co-1-V-2-P) grafts and that of the corresponding PA doped membrane.

The peak temperature (T_p) of the original ETFE film appeared at 529 °C, that of grafted ETFE film appeared at 522 °C and that of corresponding PA doped membrane appeared at 517 °C respectively. The T_p of grafted ETFE film and corresponding PA doped membrane reduces compare to that of the original ETFE film. However, TGA/DTG results indicate that co-grafting (copolymerization) of 1-VIm-co-1-V-2-P somewhat improved the thermal stability of the grafted ETFE film. Furthermore, TGA and DTG results for the membrane are in good agreement. These results to some extent also agreed with similar PVDF-g-P(N-V-2-P) membrane [15] and other reported membranes obtained by grafting various basic vinyl monomers onto fluorinated polymers [2,4,5,9,41,53]. Therefore, it can be suggested that the produced membrane is suitable for testing in a high temperature PEMFC up to 200 °C from the TGA/DTG results. It was observed that it is most likely to be thermally and physically stable from the results of TGA/DTG and stability tests conducted on the produced membrane. Therefore, it is most likely to be durable and more reliable compared to similar membranes earlier reported [2,5,8−10,15,41].

In Fig. 12, DSC thermograms of the original ETFE film, grafted ETFE film and corresponding PA doped membrane are shown. At 265.52 °C, the melting point (T_m) of the original ETFE film was captured and shifted to 265.08 °C with a coincided reduction in the melting peak area after copolymerization of 1-VIm-co-1-V-2-P. After doping of the grafted ETFE film with PA, the T_m was lowered to 264.55 °C with further reduction of
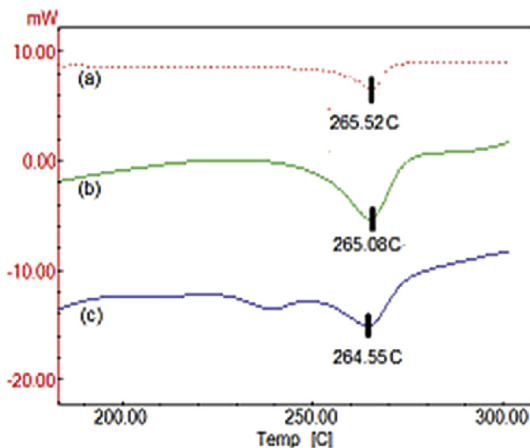

Fig. 12 − DSC thermograms of (a) original ETFE film, (b) 76% grafted ETFE film and (c) corresponding PA doped membrane.

the melting peak area. A minute partial crystal disruption developed during membrane preparation procedure (grafting and doping) suggests such a slight shift in T_m.

Furthermore, the dilution of the crystalline region of ETFE film with the amorphous P(1-VIm-co-1-V-2-P) grafts led to substantial reduction in the melting peak area. The calculated degrees of crystallinity (X_c) which showed a reduction from 34.8 to 34.2 in the original ETFE film and 33.1 in the grafted ETFE film and corresponding PA doped membrane respectively is in good agreement with this above observation. However, despite the dilution effect and minor disruption in membrane's crystalline structure. Moreover, with increasing DG(%), ETFE-g-P(1-VIm-co-1-V-2-P)/PA doped membrane shows an increase in glass transition temperature (T_g), a reasonable level of X_c was maintained.

The swelling of the membranes (water uptake from vapour phase) of the membranes was calculated according to Equation (4) and the results were plotted as depicted in Fig. 13. It is obvious that swelling percent increase as relative humidity (RH) increases. This can be adduced to the increase in the doped PA molecules as a result of the increase in the PA content. The minimum swelling percent of 8.5% was reached at 30% RH. While, the maximum swelling percent of 23.0% was attained at 80% RH. This is very close to the swelling percent of the PA doped PBI membrane at the same conditions (that is, 25% swelling at 80% RH). Thus, the swelling percent have been proven to be dependent on PA doping levels.

Acid doping kinetics

Fig. 14 presents the variation of acid doping level of membranes with doping time at different acid concentrations. It can be seen clearly that in the first 5 days the doping level increases drastically beyond which it tends to slow down as the doping time (D_t) increased. An exception to this trend occurred at acid concentration of 50%, which shows continuous progressive increasing trend. Also, an increase in the doping level at all-time intervals resulted from the rise in the acid concentration from 30% to 60%. Though, such increase was drastic when the acid concentration increased from 30%
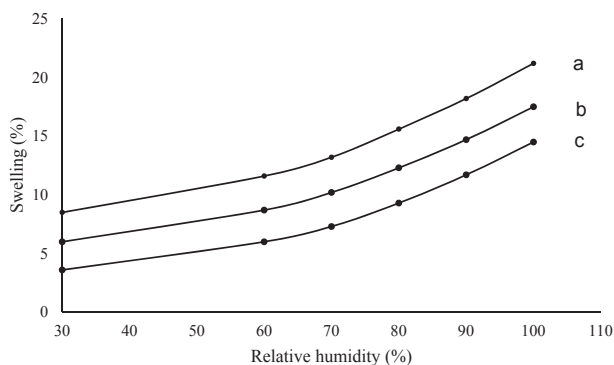

Fig. 14 − Variation of acid doping level of membranes [ETFE-g-P(1-VIm-co-1-V-2-P)] with doping time at various phosphoric acid concentrations: (a) 30%, (b) 40%, (c) 50% and (d) 60% at a constant temperature of 30 °C.

to 50% and reduced with the further increase in concentration up to 60%. These results suggest that the grafted ETFE films swell in the dopant solution (PA solution). This facilitates the doping of PA with−N−groups of the imidazole rings of the grafted P(1-VIm-co-1-V-2-P). Following a multilayer diffusion model, the reaction proceeds progressively from the surface layers towards the ETFE film core by the diffusion of the acid molecules through the grafted ETFE layers. Moreover, no variation in the doping level was observed from the increase in doping time (D_t). This observation may be attributed to the complete consumption of the available imidazole rings in the ETFE films upon achieving equilibrium. The function of every curve presented in Fig. 14 was differentiated with respect to doping time (D_t). This is done to determine the acid doping rate (dX_{PA}/dt) at various acid concentrations. Fig. 15 depicts the obtained plot of (dX_{PA}/dt) against doping time (t). As can be clearly seen, with the increase in doping time (D_t) the values of (dX_{PA}/dt) decreased drastically at all acid concentrations. This coincides with the increment in (dX_{PA}/dt) which results from the rise in the concentration of PA. This means that with the increase in doping time (t), the amount of acid adsorbed in the membrane per time unit decreases. While it increases with

Fig. 13 − Swelling (%) of the membranes from vapour phase versus relative humidity (%) for different PA doping levels: (a) 7.6, (b) 4.2 and (c) 2.3 mmol repeat polymer unit⁻¹.
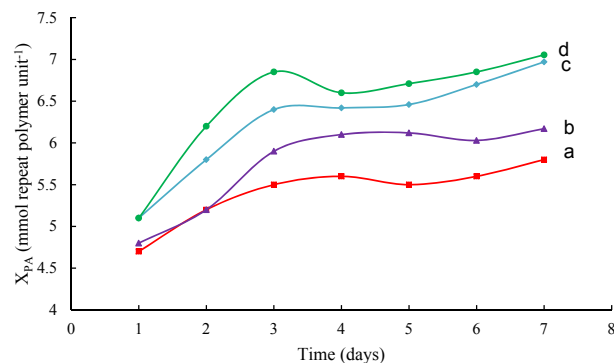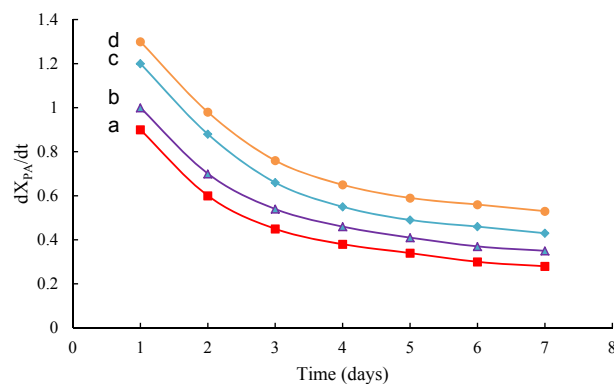

Fig. 15 − Acid doping rate of membranes [ETFE-g-P(1-VIm-co-1-V-2-P)] versus doping time for various phosphoric acid concentrations: (a) 30%, (b) 40%, (c) 50% and (d) 60% at a temperature of 30 °C.

the rise in dopant concentration and tends to slow down upon approaching equilibrium at 7 days.

In Fig. 16, the results of ionic conductivity measurements in correlation with temperature for ETFE-*g*-P(1-VIm-*co*-1-V-2-P)/PA doped membrane are shown. It was observed that conductivity of all membranes increase gradually with the increase in the temperature. The proton hopping increases as the temperature increases resulting in higher proton conductivity. Maximum conductivity value of 53 mS cm^{-1} was recorded at a combination of at 120 °C and 0% relative humidity. That is, without humidification/under dry conditions. This is an indication that the ETFE-*g*-P(1-VIm-*co*-1-V-2-P)/PA doped membrane obtained in this study is considered to be less-water dependent. Necessary to explain this trend is the understanding of the way proton conductivity occurs in acid doped membranes. Unique proton conduction mechanism of PA by self-dehydration and self-ionization enable it to exert effective proton conductivity as a dopant even in an anhydrous form. Moreover, the phosphate and imidazole moieties are often bridged by acid molecules. The effect of DG(%), DL, temperature and ionic conductivity value (σ) reported for the present ETFE-*g*-P(1-VIm-*co*-1-V-2-P)/PA doped membranes agreed to some extent with the ones reported for the ETFE-*g*-P(1-VIm) and ETFE-*g*-P(1-VIm)/TAC PA doped membranes [2,5,21,41].

For instance, measuring conductivity at the same conditions of 120 °C and 0% relative humidity, the σ values reported for the present and ETFE-*g*-P(1-VIm/TAC)/PA doped membranes were 53 mS cm^{-1} and 33 mS cm^{-1} respectively. While σ value of 140 mS cm^{-1} was reported for ETFE-*g*-P(1-VIm)/PA doped membrane at 120 °C and ~20% RH [41]. This agreed to some extent with those reported for similar heterocyclic-nitrogenous 1-VIm and 1-V-2-P based membranes [2,5,12,14—17,21,41,56].

Observably, the presence of more basic center (−N=) provided by both 1-VIm and 1- V-2-P is most probably responsible for the higher conductivity value for the present membrane. In effect, monomer(s) diffusion onto the free radicals (active sites) generated on the polymer (ETFE) backbone was enhanced leading to increased DG(%), DL and σ.

From the results of σ tests performed on the present membranes in the absence of humidification. It was observed that the σ values obtained were higher than those reported for ETFE-*g*-P(1-VIm/TAC)/PA doped membranes and

lesser than those reported earlier for ETFE-*g*-P(1-VIm)/PA doped membranes [2,5,8—10,41]The reported higher σ value for ETFE-*g*-P(1-VIm)/PA doped membrane was said to be most likely due to higher doping level (DL) and presence of water molecules within the membrane as a result of humidification which enhances proton conductivity through ETFE-*g*- P(1-VIm)/PA doped membrane [41]. While the reported lesser σ value for ETFE-*g*-P(1-VIm/TAC)/PA doped membrane was attributed to the crosslinking effect of triallyl cyanurate (TAC).

From Fig. 17 which shows the log ionic conductivity versus 1000/T, the dependence of proton conductivity of ETFE-*g*-P(1-VIm-*co*-1-V-2-P)/PA doped membrane on the temperature was found to follow Arrhenius law. The existence of a hopping-like (Grotthus) conduction mechanism existed in the membrane can be suggested based on this fact. The activation energies (E$_a$) calculated between 30 and 120 °C were found to be 2.3 kJ mol^{-1} from the Arrhenius plot. Formation of NH$^+$ proton donor sites in the membrane causing H$^+$ hopping to occur between NH$^+$ sites and PA anions along the anionic chains leading to a continuous proton transfer resulted from the doping of poly (1-VIm-*co*-1-V-2-P) grafted film with PA resulted. The results shown in Figs. 16 and 17 can be explained by putting this fact into consideration. A proton hopping via water molecules caused most probably by the presence of water in a form of bound water also contributed to proton conductivity but to a lower extent. As DL increase, the level of water molecules associated with PA by H-bonding increases.

Other PA ionic species including H$_2$PO$_4^-$ are allowed to contribute to the proton transfer by this development, consequently, a remarkable proton conductivity increment resulted. The presence of high doping level (DL) in the present membranes supported this observation. Membranes with higher DLs often exhibits higher conductivity generally, which shows that conductivity primarily depends on DLs [57]. For example, conductivity of ETFE-*g*-P(1-VIm-*co*-1-V-2-P)/PA doped membrane having DL of 7.6 mmol repeat polymer unit^{-1} was approximately 53 mS cm^{-1} at 120 °C and 0% RH, compared to conductivity value of 140 mS cm^{-1} reported for ETFE-*g*-P(1-VIm) at 120 °C and ~20% RH having DL of 6.6 mmol repeat polymer unit^{-1} [41].
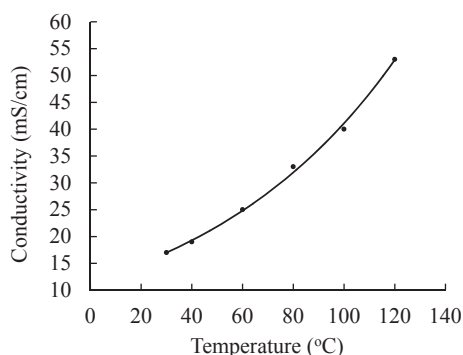

Fig. 16 — Variation in ionic conductivity of the membrane with temperature.
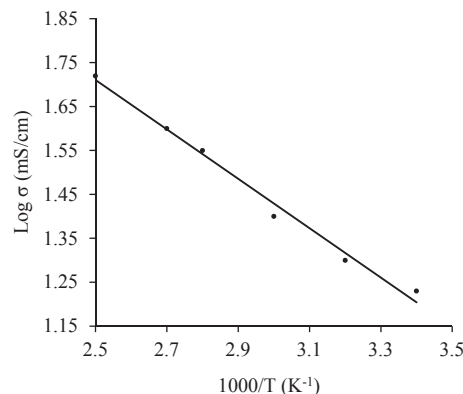

Fig. 17 — Arrhenius plot of log ionic conductivity versus reciprocal of temperature.
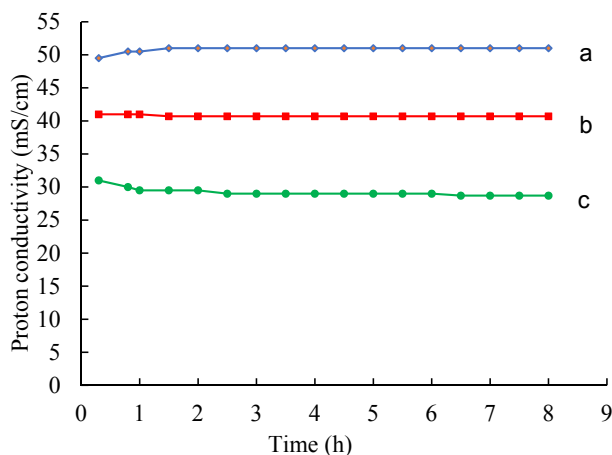
Fig. 18 − Variation of ionic conductivity in relation with time for PA doped poly (1-VIm/1-V-2-P) grafted membranes at various acid doping level (a) 7.60, (b) 4.20 and (c) 2.29 mmol repeat polymer unit^{-1} at 120 °C.

Water presence in form of bound water might also have caused a proton hopping via water molecules which contributes to proton conductivity but to a lower extent. As hopping increases with increase in temperature, a significant increase in conductivity resulted despite the fact that this membrane is a less-water dependent material. Possession of high conductivity by the present membrane is suggested by such trend. These results completely agreed with the studies that suggested that even in an anhydrous form, the PA doped membrane possesses effective proton conductivity [21,58]. Also, when PA-doped PBI membrane at 120 °C was compared with the present membrane, a similar temperature-dependent conductivity trend but with a lower conductivity value (43.4 mS cm^{-1}) was observed.

The presence of excess doped phosphoric acids having lower affinity for imidazole side chains, which possesses one imino nitrogen group permitting high level of proton mobility. Similarly, pyrrolidone side chains which contains a polar amide group and a non-polar structure allowing the pyrrolidone unit to interact favourably with PA thereby enhancing proton transport. These factors are most probably responsible for the superior conductivity values attained by the present membrane. Dissimilarly, PA doped PBI membrane in which PA is likely to have high affinity for both imino nitrogen groups of

imidazole attached to the bulk molecular chains in the PBI matrix resulting in less proton mobility. Increase in monomer(s) concentration led to substantial increase in conductivity and improved thermal stability of the produced membrane.

Thermal stability in terms of ionic conductivity loss

Membrane's stability monitored in terms of variation of ionic conductivity in correlation with time at 120 °C is shown in Fig. 18. It can be seen clearly that for all the membranes with various doping levels, there was almost no loss in proton conductivity over a time span of 8 h. This is an indication that the PA loaded sites of the membrane remain intact at the test conditions. The earlier reported TGA analysis results for a single membrane sample which has DG(%) of 54% [41]. support the TGA and DTG analyses results for the present single membrane sample which has DG(%) of 76%. Based on this observation, it can be suggested that there is a great potential in testing the produced membrane in PEM fuel cell operated over 100 °C.

In Table 1, a summary of the physicochemical properties of ETFE-*g*-P(1-VIm-*co*-1-V-2-P)/PA doped membrane compared with ETFE-*g*-P(1-VIm)/PA doped membrane, PA doped PBI and Nafion 117 membranes is presented. When ETFE-*g*-P(1-VIm-*co*-1-V-2-P)/PA doped membrane was compared with ETFE-*g*-P(1-VIm)/PA doped membrane and PA-doped PBI membranes. It can be clearly seen that it possesses an excellent combination of thermal stability and physical strength. Moreover, both ETFE-g-P(1-VIm-*co*-1-V-2-P)/PA and ETFE-*g*-P(1-VIm)/PA doped radiation-grafted membranes possess higher ionic conductivity compared to PA doped PBI membrane despite its thickness and slightly higher DL. This clearly indicates that the ETFE-*g*-P(1-VIm-*co*-1-V-2-P)/PA doped membrane obtained in this study is a promising candidate for application in high temperature PEMFCs.

XPS wide survey spectra of the original and grafted ETFE films are shown in Fig. 19. In the spectrum A of the original ETFE film, the presence of oxygen, fluorine and carbon in the forms of O1s, F1s and C1s at 532.0, 688.0 and 285.0 eV respectively can be seen clearly. The presence of undisclosed additives that were used in the processing of the ETFE film during manufacturing is most likely responsible for the presence of oxygen in the original ETFE film. An additional nitrogen related new peak (N1s) appeared at 401.0 eV which was attributed to the imine group of the imidazole ring and amide

Table 1 − Summary of the physicochemical properties of ETFE-*g*-P(1-VIm-*co*-1-V-2-P)-PA doped membranes compared with PA doped PBI and Nafion 117 membranes.

Membrane properties	P(1VIm-*co*-1-V-2-P)	P1VIm/PA	PBI/PA	Nafion 117
Degree of grafting (wt%)	76	54	N/A	N/A
Doping level (mmol repeat polymer unit^{-1})	7.6	6.6	5.7[4]	N/A
Thickness of dry membrane (μm)	170	130	100[13]	183[14]
Conductivity at 120 °C (mS cm^{-1})	53	140	9.6[4]	85[14]
Thermal stability (°C)	Above 200	Up to 200	−	120[16]
Melting temperature (°C)	264	261	−	350[16]
Degree of crystallinity (%)	33.1	25.2	−	17.7[17]

PA: phosphoric acid; PBI: polybenzimidazole; P(1-VIm): poly-1-vinylimidazole; P(1-V-2-P): poly-1-vinyl-2-pyrrolidone.
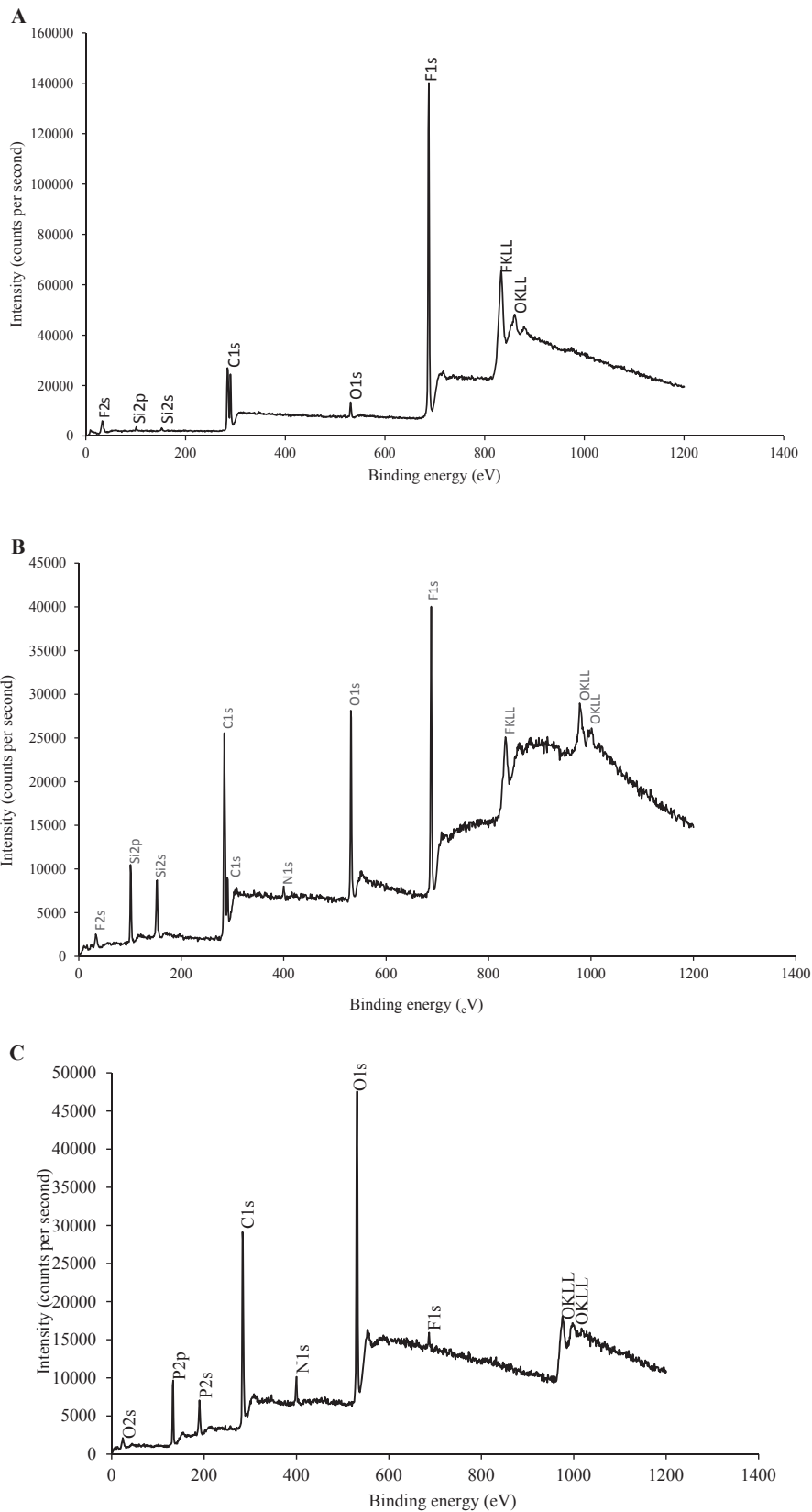
Fig. 19 — XPS wide scan spectra of: (A) original ETFE film and (B) 76% grafted ETFE film and (C) corresponding PA doped membrane.

group of the pyrrolidone ring belonging to the poly (1-VIm-co-1-V-2-P) grafted film, that is, ETFE-g-P(1-VIm-co-1-V-2-P) is contained in spectrum B [2,15]. Furthermore, as depicted in the spectrum C′, PA doped membrane shown other additional new bands resembling P (P2p and P2s) appeared at 133.0 and 190.0 eV, respectively. These results, on one hand, provide solid supporting evidence for the grafting of 1-VIm and 1-V-2-P onto ETFE film. It also proved beyond reasonable doubt the grafting of poly (1-VIm-co1-V-2-P) chains onto EB-preirradiated ETFE films and subsequent PA incorporation through membranes' doping were highly successful. On the other hand, these results are in a good concord with similar results of XPS analysis of PA doped (nanoimpregnated) membranes that were reported in literature [2,38].

Conclusion

ETFE-g-P(1-VIm-co-1-V-2-P)/PA doped high temperature proton conducting membrane (HT-PCM) for high temperature proton exchange membrane fuel cell (HT-PEMFC) have been synthesized by co-grafting (copolymerization) of 1-VIm and 1-V-2-P onto EB-preirradiated films using RIG method. Copolymerization of 1-V-2-P and 1-VIm (1-VIm-co-1-V-2-P) led to higher DG(%) and DL compared to grafting of only 1-VIm onto ETFE film and subsequent PA doping [ETFE-g-P(1-VIm)/PA] doped membrane. However, lower ionic conductivity values were obtained compare to the conductivity values reported for similar ETFE-g-P(1-VIm)/PA-doped membrane at different conditions (120 °C and ~20% relative humidity) [5,28].

Furthermore, ETFE-g-P(1-VIm)/PA and ETFE-g-P(1-VIm-co-1-V-2-P)/PA doped membranes were compared in terms of thermal stability and physical strength. Membrane prepared in this study possess the following impressive properties: it is thermally and chemically stable above 200 °C. It has reasonable level of crystallinity sufficient to maintain the mechanical stability required for its use as HT-PEM in HT-PEMFC. Conductivity of 53 mS cm^{-1} at 120 °C and 0% relative humidity. That is, without humidification/under dry conditions was achieved and conductivity of the membrane increased with an increase in temperature.

The overall results indicate that the produced membrane is conductive despite the fact that conductivity was measure under dry conditions and being less-water dependent. It possesses impressive combination of chemico-physical properties which qualified it for testing in HT-PEMFC test station above 100 °C. Therefore, it is appealing for application in PEMFC above 100 °C.

Comparing ETFE-g-P(1-VIm)/PA and ETFE-g-P(1-VIm-co-1-V-2-P)/PA doped membranes. The latter had higher DG(%) and DL. However, the former had superior ionic conductivity value. Probably, because conductivity of the former was measured under humidified conditions. The latter is better in terms of thermal stability and physical strength. For both, DG(%), DL and ionic conductivity values increase with an increase in monomer(s) concentration. It is the belief of the authors that when fuel cell test, durability and other tests are successfully performed on the obtained membrane using HT-PEMFCs test station. Additional impressive combination of its chemico-physical properties will be obtained. Some desirable

requirements that must be possess by PEM meant for HT-PEMFC including trade-off between proton conductivity, thermal stability and physical strength was achieved by the produced PA doped membrane, besides being less-water dependent.

In conjunction with reaction parameters, the kinetics of RIGC of 1-VIm-co-1-V-2-P onto ETFE films was studied. It was observed that reaction parameters, such as, M, RT and D determines the reaction kinetics. A quantitative kinetic description for r_{p0}, γ and t_0 on the reaction parameters studied was obtained from the experimental data that were fitted to a simple mathematical model selected. Particularly, the R_g dependence on M and D were found to be 3.39 and 2.23 respectively. Therefore, it was observed that chemico-mechanical effect most likely strongly influence the grafting of 1-VIm-co-1-V-2-P onto ETFE films. It can also be reasonably suggested that the initial grafting rate is low and strongly depends on RT based on the higher E_a of 116.40 kJ/mol obtained for this grafting reaction. In the present research work, a better understanding of homogenous membranes preparation from ETFE films for HT-PEMFC has emerged from the comprehensive kinetic studies which described the grafting of 1-VIm-co-1-V-2-P onto EB-preirradiated ETFE films, that is, ETFE-g-P(1-VIm-co-1-V-2-P). By proper selection of reaction conditions and parameters, control and tuning of the DG(%) can be achieved easily.

List of abbreviations

1-VIm	1-Vinylimidazole
1-V-2-P	1-Vinyl-2-pyrrolidone
N-VIm	N-Vinylimidazole
2-V-P	2-Vinyl pyridine
4-V-P	4-Vinyl pyridine
A	Pre-exponential factor or frequency factor
ATR	Attenuated total reflectance
co	Copolymerization
D	Absorbed dose
DG(%)	Degree of grafting
DSC	Differential scanning calorimetry
DT	Doping temperature
Dt	Doping time
DTG	Differential/first derivative thermogravimetric
EB	Electron beam
ETFE	Poly(ethylene-alt-tetrafluoroethylene)
ETFE-g-P(1-VIm)	ETFE films grafted with poly(1-vinylimidazole)

ETFE-g-P(1-V-2-P)	ETFE films grafted with poly(1-vinyl-2-pyrrolidone)
FEP	Poly(tetrafluoroethylene-co-hexafluoropropylene)
FTIR	Fourier transform infrared spectroscopy
g	Grafted
GT	Grafting temperature
Gt	Grafting time
HCl	Hydrochloric acid
HT-PEMFC	High temperature polymer electrolyte fuel cell
IEC	Ion exchange capacity
LDPE	Low density polyethylene
M	Monomer concentration
NVF	N-Vinylformamide
NVP	N-vinyl-2-pyrrolidone
PA	Phosphoric acid
PBI/H_3PO_4	Phosphoric acid-doped Poly(benzimidazole)
PCMs	Proton conducting membranes
PE	Polyethylene
PEMs	Proton exchange membrane
PEMFC	Proton exchange membrane fuel cell
PES	Poly (ether sulfone)
PO	Propylene oxide
PTFE	Polytetrafluoroethylene
PVDF	Poly (vinylidene fluoride)
R_g	Grafting rate
RIG	Radiation induced grafting
RIGC	Radiation induced graft copolymerization
RT	Reaction temperature
Rt	Reaction time
S_{ty}	Solvent type
TGA	Thermogravimetric analysis
VP	Vinyl pyrrolidone

List of symbols

A	Area (m^2)
DG(%)	Degree of grafting (wt%)
E_a	Activation energy
ΔH_m	Heat of melting of ETFE film ($J°g^{-1}$)
$\Delta H_{m\,100}$	Heat of melting of 100% crystalline ETFE polymer ($J°g^{-1}$)
k	Rate constant
k_p	Polymerization rate constant ($L°mol^{-1}\,s^{-1}$)
k_t	Rate constant of bimolecular termination ($L°mol^{-1}\,s^{-1}$)
L	Distance between probes (cm)
w_g	Weight of the grafted film (g)
w_o	Weight of the original ETFE film (g)
$[\mathbf{M}]_0$	Monomer concentration (vol%)
M_d	Molar mass of phosphoric acid ($g\,mol^{-1}$)
M_p	Molar mass of polymer repeat unit ($g\,mol^{-1}$)
$[\mathbf{P^•}]_0$	Initial radical concentration
r_{p0}	Initial polymerization rate
R	Gas constant = 8.314 ($J\,K^{-1}\,mol^{-1}$)
R	Resistance (Ω)
t_0	Delay time
T	Thickness of the membrane sample (cm)
T	Temperature (°C)
T	Absolute temperature (K)
T^{-1}	Reciprocal of absolute temperature (K^{-1})
T_g	Glass transition temperature (°C)

T_m	Melting temperature (°C)
T_p	Peak temperature (°C)
T_{onset}	Onset temperature of degradation (°C)
W	Width of the membrane (cm)
w_d	Mass fraction of dopant (g)
w_i	Percentage of weight increase of the grafted ETFE film
W_{dry}	Weight of dry membrane (g)
w_g	Weight of the grafted ETFE film (g)
w_o	Weight of the original ETFE film (g)
W_{wet}	Weight of the swelled membrane (g)
X_c	Degree of crystallinity
X_{PA}	Acid doping level per repeated unit of polymer (mmol repeat $unit^{-1}$)
γ	Characteristic radical recombination rate
σ	Proton conductivity ($S°cm^{-1}$)

REFERENCES

[1] Sithambaranathan P, Nasef MM, Ahmad A. Kinetic behaviour of graft copolymerisation of nitrogenous heterocyclic monomer onto EB-irradiated ETFE films. J Radioanal Nucl Chem 2015:1—10.

[2] Nasef MM, Saidi H, Ahmad A, Ahmad Ali A. Optimization and kinetics of phosphoric acid doping of poly(1-vinylimidazole)-graft-poly(ethylene-co-tetrafluorethylene) proton conducting membrane precursors. J Membr Sci 2013;446:422—32.

[3] Nasef MM, Saidi H, Uthman H, Sithambaranathan P. Advances in membranes for high temperature polymer electrolyte membrane fuel cells. In: Inamuddin, editor. Advanced functional polymers and composites: materials, devices and allied applications. New York: Nova Science Publishers, Inc.; 2013. p. 1—44.

[4] Aly-Ibrahim AA. Proton conducting membrane by radiation-induced grafting of 1-vinylimidazole onto poly (ethylene-co-tetrafluoroethylene) film and phosphoric acid doping. Skudai: Universiti Teknologi Malaysia; 2012.

[5] Nasef MM, Aly AA, Saidi H, Ahmad A. Optimization of reaction parameters of radiation induced grafting of 1-vinylimidazole onto poly(ethylene-co-tetraflouroethene) using response surface method. Radiat Phys Chem 2011;80:1222—7.

[6] Nasef MM, Saidi H, Mohd Dahlan KZ. Kinetic investigations of graft copolymerization of sodium styrene sulfonate onto electron beam irradiated poly (vinylidene fluoride) films. Radiat Phys Chem 2011;80:66—75.

[7] Asensio JA, Sánchez EM, Gómez-Romero P. Proton-conducting membranes based on benzimidazole polymers for high-temperature PEM fuel cells. A chemical quest. Chem Soc Rev 2010;39:3210—39.

[8] Schmidt C, Schmidt-Naake G. Proton conducting membranes obtained by doping radiation-grafted basic membrane matrices with phosphoric acid. Macromol Mater Eng 2007;292:1164—75.

[9] Schmidt C, Schmidt-Naake G. Grafting of 1-vinylimidazole onto pre-irradiated ETFE films. Macromol Mater Eng 2007;292:1067—74.

[10] Schmidt C, Schmidt-Naake G. Fe^{2+} catalyzed synthesis of radiation grafted functional membranes and application in fuel cells and ion recovery. Macromol Symp 2007;259:181—7.

[11] Haaf F, Sanner A, Straub F. Polymers of N-Vinylpyrrolidone: synthesis, characterization and uses. Polym J 1985;17:143—52.

[12] Martínez-Piña F, Gargallo L, Radić D. N-vinylimidazole-N-vinyl-2-pyrrolidone copolymers. Part I. Reactivity ratios, solubility and viscosimetric study. Polym Int 1998;47:340–4.

[13] Jacob S. Polymer-supported solid phase reactions using N-vinylpyrrolidone derived polymers. Kottayam, Kerala, India: Mahatma Ghandi University; 2006.

[14] Parambil AM, Puttaiahgowda YM, Shankarappa P. Copolymerization of N-Vinyl pyrrolidone with methyl methacrylate by Ti (III)-DMG redox initiator. Turkish J Chem 2012;36:397–409.

[15] Xu C, Huang W, Zhou Y, Yan D, Chen S, Huang H. Graft copolymerization of N-vinyl-2-pyrrolidone onto pre-irradiated poly(vinylidene fluoride) powder. Radiat Phys Chem 2012;81:426–31.

[16] Djelloul B, Abdelkader R, Issam FM, Mohammed B. Synthesis, characterization and kinetics studies of block copolymer consist on N-vinyl-2-pyrrolidone and propylene oxide catalysed by Maghnite-H (Algerian MMT). Int J Chem Mater Sci 2013;1:201–9.

[17] Arosio P, Mosconi M, Storti G, Banaszak B, Hungenberg KD, Morbidelli M. Precipitation copolymerization of Vinyl-imidazole and Vinyl-pyrrolidone, 2–kinetic model. Macromol React Eng 2011;5:501–17.

[18] Arosio P, Mosconi M, Storti G, Morbidelli M. Precipitation copolymerization of Vinyl-Imidazole and Vinyl-Pyrrolidone, 1–experimental analysis. Macromol React Eng 2011;5:490–500.

[19] Sanli L, Gürsel SA. High temperature proton exchange membranes for fuel cells by radiation grafting. In: Meeting abstracts: the electrochemical society; 2010. p. 834.

[20] Şanlı LI, Alkan Gürsel S. Synthesis and characterization of novel graft copolymers by radiation-induced grafting. J Appl Polym Sci 2011;120:2313–23.

[21] Sanlı L, Tas S, Yürüm Y, Gürsel S. Water free operated phosphoric acid doped radiation-grafted proton conducting membranes for high temperature polymer electrolyte membrane fuel cells. Fuel Cells 2014;14:914–25.

[22] Wainright J, Wang JT, Weng D, Savinell R, Litt M. Acid-doped polybenzimidazoles: a new polymer electrolyte. J Electrochem Soc 1995;142. L121–L3.

[23] Nasef MM. Proton exchange membranes by radiation-induced graft copolymerisation of styrene onto fluorinated polymers. Skudai: Universiti Teknologi Malaysia; 1999a.

[24] Nasef MM, Hegazy E-SA. Preparation and applications of ion exchange membranes by radiation-induced graft copolymerization of polar monomers onto non-polar films. Prog Polym Sci 2004;29:499–561.

[25] Kirsh YE, Kirsh IUĖ. Water soluble poly-N-vinylamides: synthesis and physicochemical properties. John Wiley & Sons; 1998.

[26] Dupuis A-C. Proton exchange membranes for fuel cells operated at medium temperatures: materials and experimental techniques. Prog Mater Sci 2011;56:289–327.

[27] Chen W, Sun G, Guo J, Zhao X, Yan S, Tian J, et al. Test on the degradation of direct methanol fuel cell. Electrochim Acta 2006;51:2391–9.

[28] Hogarth WH, Da Costa JD, Lu GM. Solid acid membranes for high temperature (¿ C) proton exchange membrane fuel cells. J Power Sources 2005;142:223–37.

[29] Karimi G, Baschuk J, Li X. Performance analysis and optimization of PEM fuel cell stacks using flow network approach. J Power Sources 2005;147:162–77.

[30] Ben Youcef H. Radiation grafted ETFE based membranes for fuel cells. In: Diss., Eidgenössische Technische Hochschule ETH Zürich, Nr. 18215; 2009. p. 2009.

[31] Kallitsis JK, Geormezi M, Neophytides SG. Polymer electrolyte membranes for high-temperature fuel cells based on aromatic polyethers bearing pyridine units. Polym Int 2009;58:1226–33.

[32] Kang K, Kang PH, Nho YC. Preparation and characterization of a proton-exchange membrane by the radiation grafting of styrene onto polytetrafluoroethylene films. J Appl Polym Sci 2006;99:1415–28.

[33] Kallio T. Electrochemical and physicochemical characterization of radiation-grafted membranes for fuel cell. PhD Thesis. 2003. p. 1–35.

[34] Kerres JA. Development of ionomer membranes for fuel cells. J Membr Sci 2001;185:3–27.

[35] Vilčiauskas L, Tuckerman ME, Bester G, Paddison SJ, Kreuer K-D. The mechanism of proton conduction in phosphoric acid. Nat Chem 2012;4:461–6.

[36] Wallasch F. Investigations on radiation grafted polymer fuel cell membranes: preparation, characterization, application. Zürich (ETHZ): Swiss Federal Institute of Technology; 2010.

[37] Wang S, Zhao C, Ma W, Zhang G, Liu Z, Ni J, et al. Preparation and properties of epoxy-cross-linked porous polybenzimidazole for high temperature proton exchange membrane fuel cells. J Membr Sci 2012;411:54–63.

[38] Xu C. Development of membranes for low and intermediate temperature polymer electrolyte membrane fuel cell. London: Newcastle University UK; 2013.

[39] Nasef MM, Saidi H. Preparation of crosslinked cation exchange membranes by radiation grafting of styrene/divinylbenzene mixtures onto PFA films. J Membr Sci 2003;216:27–38.

[40] Ślaski MW. Radiation grafted fuel cell membranes with improved oxidative stability. Poland: Warsaw University of Technology; 2007.

[41] Nasef MM, Ali AA, Saidi H. Composite proton conducting membrane by radiation-induced grafting of 1-vinylimidazole onto poly(ethylene-co-tetrafluoroethylene) and phosphoric acid doping. High Perform Polym 2012;10:1–7.

[42] Gubler L, Scherer GG. Advanced polymer science. Berlin, Heidelberg: Springer-Verlag Limited; 2008.

[43] Dambatta B, Ebdon J. Kinetic studies of free-radical polymerizations of I-vinylimidazole initiated by benzoyl peroxide and azoisobutyronitrile. Eur Polym J 1986;22:783–6.

[44] Chapiro A. Peculiar aspects of the free-radical polymerization of 1-vinylimidazole. Int J Radiat Appl Instrum Part C Radiat Phys Chem 1992;40:89–93.

[45] Gürsel SA, Wokaun A, Scherer GG. Influence of reaction parameters on grafting of styrene into poly (ethylene-alt-tetrafluoroethylene) films. Nucl Instrum Methods Phys Res Sect B Beam Interact Mater Atoms 2007;265:198–203.

[46] Hogarth WHJ, Diniz da Costa JC, Lu GQ. Solid acid membranes for high temperature (>140 °C) proton exchange membrane fuel cells. J Power Sources 2005;142:223–37.

[47] Lepit A, Aini N, Jaafar N, Hashim N, Ali A, Dahlan K, et al. Influences of co-polymerization 1-vinylimidazole onto γ-irradiated poly (vinylidene flouride) membranes. Int J Electrochem Sci 2012;7:8560–77.

[48] Nasef MM, Saidi H, Dahlan KM. Comparative investigations of radiation-grafted proton-exchange membranes prepared using single-step and conventional two-step radiation-induced grafting methods. Polym Int 2011;60:186–93.

[49] Liang J, Huang Y, Zhang L, Wang Y, Ma Y, Guo T, et al. Molecular-level dispersion of graphene into poly (vinyl alcohol) and effective reinforcement of their nanocomposites. Adv Funct Mater 2009;19:2297–302.

[50] Nasef MM, Saidi H. Structure of polyethylene-graft-polystyrene sulfonic acid membranes prepared by radiation-induced grafting. Int J Polym Mater 2004;53:1027–43.

[51] Gürsel SA, Wokaun A, Scherer GG. The influence of crosslinker on the properties of radiation-grafted films and membranes based on ETFE. J Membr Sci 2008;311:208–15.

[52] Li J, Sato K, Ichiduri S, Asano S, Ikeda S, Iida M, et al. Pre-irradiation induced grafting of styrene into crosslinked and non-crosslinked polytetrafluoroethylene films for polymer electrolyte fuel cell applications. I: influence of styrene grafting conditions. Eur Polym J 2004;40:775–83.

[53] Kawahara M, Morita J, Rikukawa M, Sanui K, Ogata N. Synthesis and proton conductivity of thermally stable polymer electrolyte: poly (benzimidazole) complexes with strong acid molecules. Electrochim Acta 2000;45:1395–8.

[54] Vhathvarothai N, Ness J, Yu QJ. An investigation of thermal behaviour of biomass and coal during copyrolysis using thermogravimetric analysis. Int J Energy Res 2014;38:1145–54.

[55] Ramimoghadam D, Hussein MZB, Taufiq-Yap YH. The effect of sodium dodecyl sulfate (SDS) and cetyltrimethylammonium bromide (CTAB) on the properties of ZnO synthesized by hydrothermal method. Int J Mol Sci 2012;13:13275–93.

[56] Haddadi-Asl V, Burford RP, Garnett JL. Radiation graft modification of N-Vinyl-2-pyrrolidone onto ethylene-propylene rubber. Iran J Polym Sci Technol 1995;4:170–9.

[57] Yang J, Aili D, Li Q, Cleemann LN, Jensen JO, Bjerrum NJ, et al. Covalently cross-linked sulfone polybenzimidazole membranes with poly(Vinylbenzyl Chloride) for fuel cell applications. ChemSusChem 2013;6:275–82.

[58] Nasef MM, Shamsaei E, Saidi H, Ahmad A, Dahlan KZM. Preparation and characterization of phosphoric acid composite membrane by radiation induced grafting of 4-vinylpyridine onto poly(ethylene-co-tetrafluoroethylene) followed by phosphoric acid doping. J Appl Polym Sci 2013;10:1–9.